Supporting Information

Rational Design of Galvanically Replaced Pt-Anchored Electrospun WO_3 Nanofibers as Efficient Electrode Materials for Methanol Oxidation

Zhi-gang Zhao,* Zhao-Jun Yao, Jing Zhang, Rui Zhu, Yu Jin, Qing-wen Li*

Suzhou Institute of Nano-Tech and Nano-Bionics,
Ruoshui Road 398, Suzhou 215123, China

[1] Experimental details:

Characterization: X-ray diffraction (XRD) patterns of the prepared samples were recorded on a Bruker AXS D8 Advance X-ray diffractometer with a Cu Kα radiation target (40 kV, 40 mA). The N_2 sorption measurement was performed using Micromeritics ASAP2020 at 77 K, and the specific surface area and the pore size distribution were calculated using the Brunauer Emmett Teller (BET) and Barrett Joyner Halenda (BJH) methods, respectively. Field emission scanning electron microscopy (FE-SEM) analysis was performed on a FEI Quanta 400 FEG field emission scanning electron microscope. Transmittance electron microscopy (TEM) images were obtained on a FEI Tecnai G2 F20 S-Twin electron microscope operating at 200 kV. Energy-dispersive X-ray spectra (EDS) were collected from an attached Apollo 40 SDD energy-dispersive spectrometer fixed on a FEI Quanta 400 FEG field emission scanning electron microscope.

Electrochemical measurements: Cyclic voltammetry and chronoamperometry were performed on a CHI605D Electrochemical Analyzer. The measurements were made using a three electrode cell set up. An Ag/AgCl, saturated KCl electrode and a Pt foil were used as reference and counter electrodes, respectively. WO_3-supported Pt nanoparticles and carbon nanotubes are mixed and stirred in DMF solution. Then a known amount of the dispersion was transferred onto a glassy carbon electrode as a working electrode, and dried slowly under irradiation with incandescent light. A solution of 1M CH_3OH in 1M H_2SO_4 was used to study the methanol oxidation activity. All the electrochemical studies were performed at a scan rate of $25mVs^{-1}$. Pt loading used in all samples is 60 $\mu g/cm^2$ and the geometric area of the working electrode is 0.07 cm^2.

.

[2] Nitrogen adsorption-desorption isotherm plot of electrospun WO_3 nanofibers and commercial WO_3 particles:

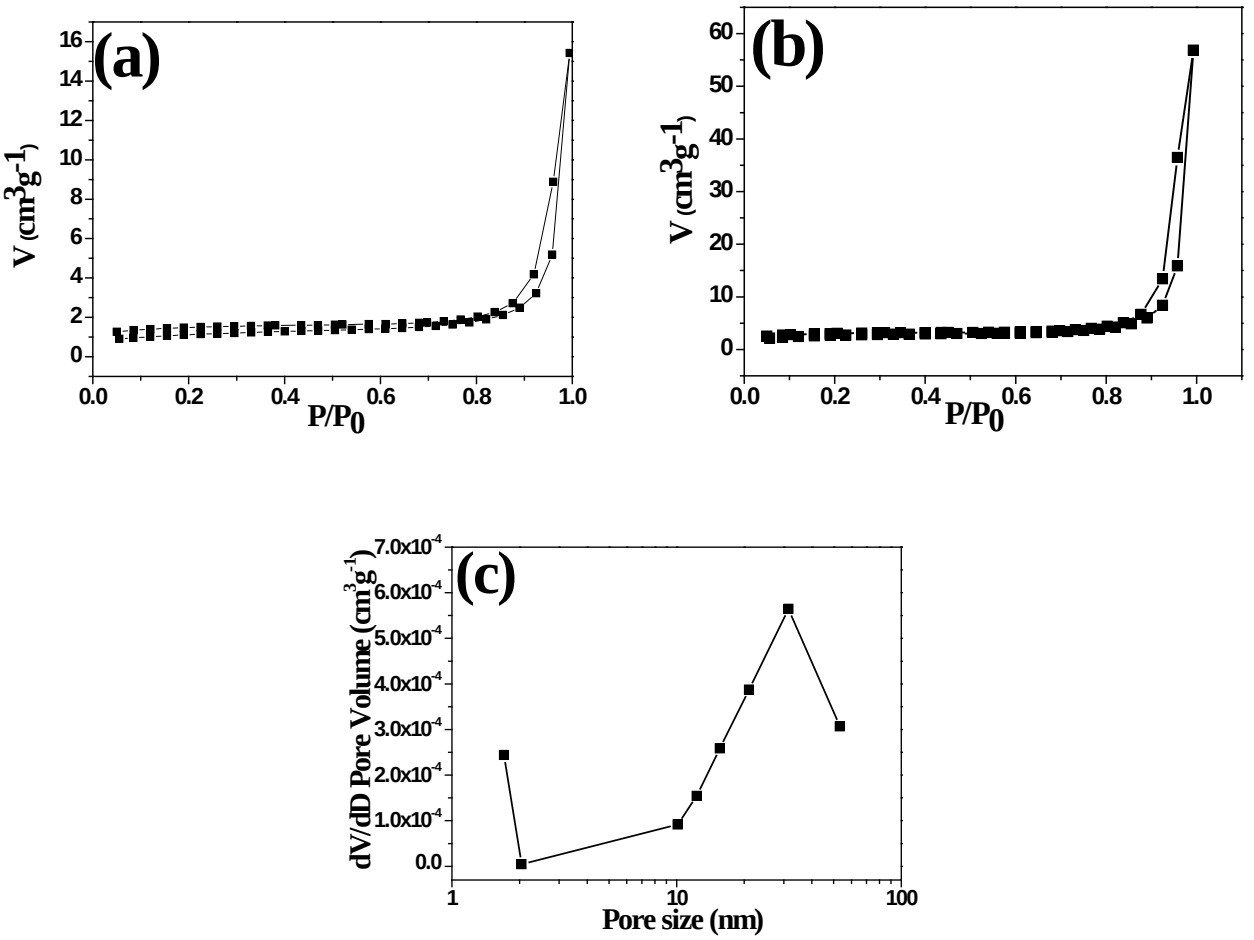

Figure S1: Nitrogen adsorption-desorption isotherm plot of (a) commercial WO_3 and (b) WO_3 nanofibers, and (c) Barrett-Joyner-Halenda (BJH) pore size distribution plot of WO_3 nanofibers.

Commercial WO_3 particles are found to have only a low BET surface area of about 3-4 m^2g^{-1}. However, According to Tuan-Anh Nguyen et al.' studies (Materials Letters 65 (2011) 2823–2825) and our studies, the specific surface area of electrospun WO_3 nanofibers of different diameters can reach up to about 10-40 $m^2g\text{-}^1$, which is much larger than that of commercial WO_3 particles. Moreover, the pore-size distribution plot indicates the electrospun WO_3 nanofibers contain a large number of mesopores, which could be attributed to the inter-gain space within the nanofibers (Materials Letters 65 (2011) 2823–2825).

[3] Schematic illustration of Pt nanoparticle deposition on tungsten oxide nanofibers and carbon nanotubes

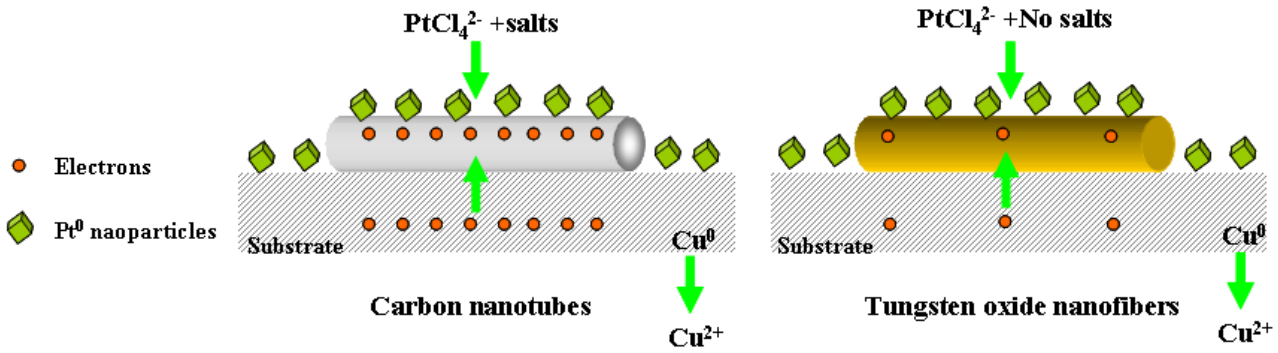

Figure S2: Schematic illustration of Pt nanoparticle deposition on tungsten oxide nanofibers and carbon nanotubes

[4] Energy-dispersive X-ray spectroscopy and X-ray diffraction pattern of Pt nanocubes and nanospheres-decorated WO_3 nanofibers:

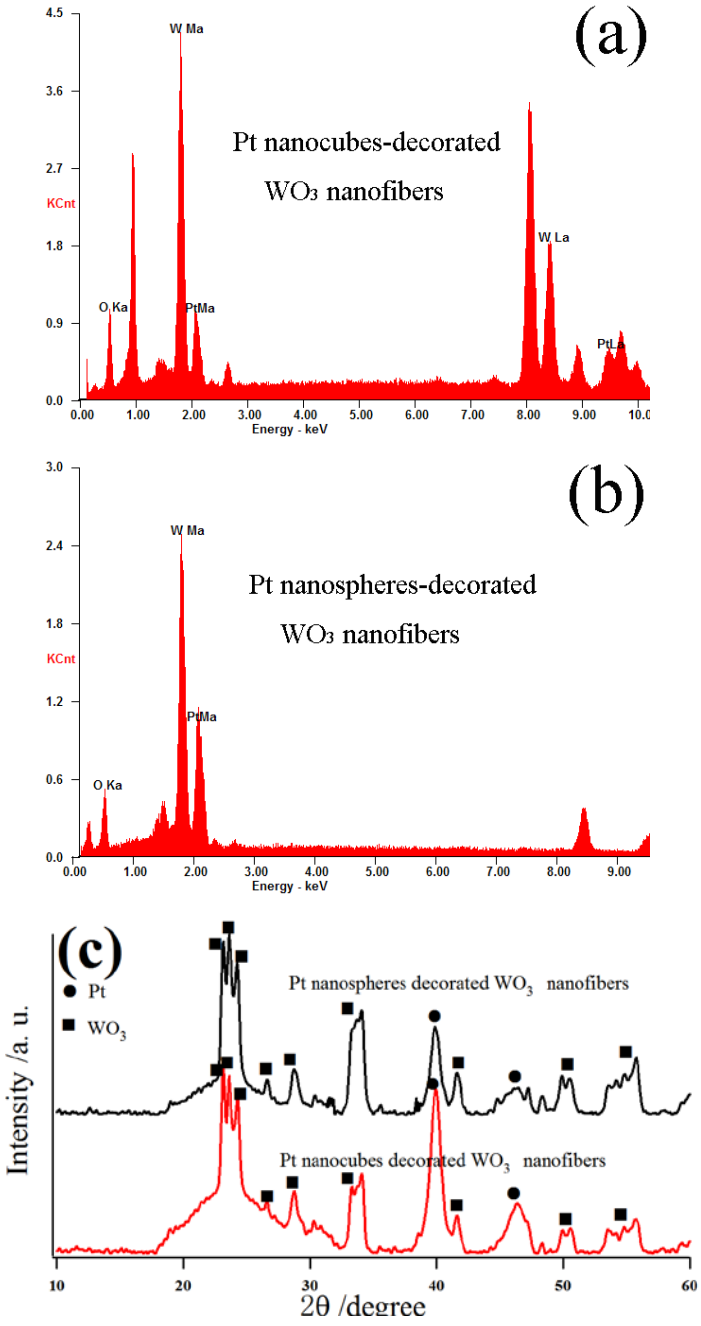

Figure S3: Energy-dispersive X-ray spectroscopy (a, b) and X-ray diffraction patterns (c) of Pt nanocubes and nanospheres-decorated WO_3 nanofibers

[5] SEM images of commercial WO_3 particles decorated with and without Pt naoparticles:

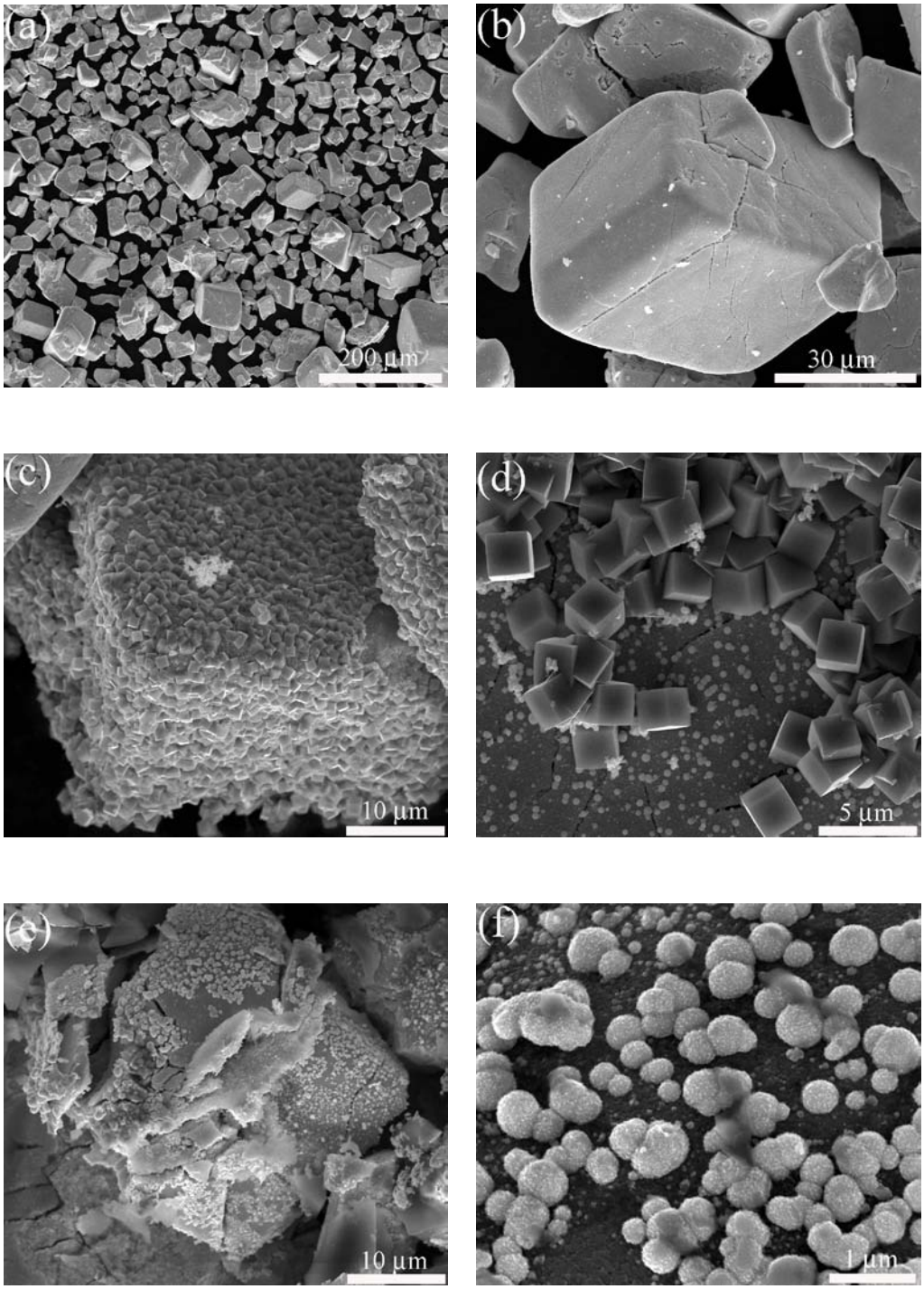

Figure S4: SEM images of (a, b) commercial WO_3 particles; (c, d) Pt nanocubes-deposited commercial WO_3 particles; (e, f) Pt nanospheres-deposited commercial WO_3 particles.